

# Erosion-creep-collapse mechanism of underground soil loss for the karst rocky desertification in Chenqi village, Puding county, Guizhou, China

Jianxiu Wang · Baoping Zou · Yan Liu ·  
Yiqun Tang · Xinbao Zhang · Ping Yang

Received: 25 May 2013 / Accepted: 22 February 2014  
© Springer-Verlag Berlin Heidelberg 2014

**Abstract** Carbonate rocks distribute widely in China. The total area of the carbonate rocks is about 3,430,000 km<sup>2</sup>, and the exposed area of the carbonate is approximately 13 % of China's territory. In 2003, soil loss in Yunnan, Guizhou, and Guangxi provinces reached 179,600 km<sup>2</sup>, which is almost 40.1 % of the total area, causing rocky desertification. In this study, the erosion-creep-collapse mechanism of underground soil loss for the karst rocky desertification in Chenqi village, Puding county, Guizhou province is proposed. The mechanism occurs under the following geological environment: slope surface undulation, underlying bedrock surface fluctuation and thin and inhomogeneous soil overlying, overlying soil generation by bedrock weathering, underground karst development, and large groundwater depth and lying water table under the bottom of soils. The erosion-creep-collapse mechanism of underground soil loss in the karst slopes is explained as follows: power loss due to human cultivation activities that destroy the soil structure, hydraulic force formed by rainfall infiltration, wet–dry cycle generated by rainfall, erosion effect caused by rainfall penetration, creeping and flowing of plastic-stream soil, and collapse. The erosion-creep-collapse mechanism of underground soil

loss has seven steps: disturbance of soils filled in underground karst cave by human activities, internal soil erosion and partial collapse caused by hydraulic power, internal free surface formation within the soil in the filled karst cave, internal soil creeping, soil pipe formation, soil pipe collapse, and ground surface collapse and filling. Soil loss develops slowly, and sudden transportation occurs by collapse. Soil loss can be explained by the proposed mechanism, and soil loss can be prevented by controlling soil collapse.

**Keywords** Karst rocky desertification · Underground soil loss · Erosion-creep-collapse mechanism

## Introduction

Carbonate rocks distribute widely in China. The total area of the carbonate rocks is about 3,430,000 km<sup>2</sup>, and the exposed area of the carbonate is approximately 13 % of China's territory (Chinese Academy of Sciences, Institute of Karst Geology Research Group 1979). They are mainly distributed in Yunnan, Guizhou, and Guangxi provinces. In 2003, soil loss in these three provinces reached 179,600 km<sup>2</sup>, which is almost 40.1 % of the total area. The loss of the soil may cause rocky desertification (Wang 2003), and karst rocky desertification (Fig. 1) is a typical type of land degradation in the Southwestern China. The karst rock desertification has great ecological and economical implications on the local people (Huang and Cai 2007). To the end of 2011, the total land area of karst rocky desertification was 12.002 million hectares, which is about 26.5 % of karst land area and 11.2 % of regional land area. 455 counties and 5,575 townships in Hubei, Hunan, Guangdong, Guangxi, Chongqing, Sichuan, Guizhou, and

---

J. Wang · Y. Tang · P. Yang  
Key Laboratory of Geotechnical and Underground Engineering  
of Ministry of Education, Tongji University,  
Shanghai 200092, China

J. Wang (✉) · B. Zou · Y. Liu · Y. Tang · P. Yang  
Department of Geotechnical Engineering, Tongji University,  
Shanghai 200092, China  
e-mail: wang\_jianxiu@163.com

X. Zhang  
Institute of Mountain Hazards and Environment, Chinese  
Academy of Sciences, Chengdu 610041, China



**Fig. 1** Karst rocky desertification in Guizhou province (1999 Institute of Karst Geology)

**Table 1** Distribution area of rocky desertification-affected land in the karst mountain in Southwest China (State Forest Administration P.R. China 2012)

| Province (autonomous region or municipality) | Total (km <sup>2</sup> ) | Percentage of total rocky desertification area (%) |
|--|--------------------------|--|
| Guizhou                                      | 30,240                   | 25.2   |
| Guangxi                                      | 19,260                   | 16.0   |
| Guangdong                                    | 640                      | 0.5  |
| Yunnan                                       | 28,400                   | 23.7   |
| Sichuan                                      | 7,320                    | 6.1  |
| Chongqing                                    | 8,950                    | 7.5  |
| Hunan  | 14,310                   | 11.9   |
| Hubei  | 10,910                   | 9.1  |

Yunnan provinces (autonomous regions and municipalities) are affected by the karst rock desertification (State Forest Administration P.R. China 2012). See Table 1.

In recent years, a series of active exploration and research on many aspects, such as the soil loss mechanisms (Geissen et al. 2007; Zhang et al. 2007a, b, 2011; Yang et al. 2011a, b; Ye et al. 2011; Peng and Wang 2012; Zhou et al. 2012a, b), the prediction models (Peng et al. 2007; Yang et al. 2010; Wang et al. 2010; Febles-González et al. 2012; Zhou et al. 2012a, b), the loss soil area quantifying (Anselmetti et al. 2007), the evaluating (Kheir et al. 2008; Vega and Febles 2008; Febles et al. 2009; Feeser and O'Connell 2009; Xu et al. 2009), the environmental effects (Chen et al. 2009; Zhang et al. 2010; Xu et al. 2011; Yang et al. 2011a, b; Jiang et al. 2013) and the impact factors (Xu et al. 2008) have been conducted. However, these researches did not explain where the lost soil is transported and accommodated. The karst erosion is too slow to provide enough space. For example, approximately 863.7 km<sup>2</sup> of exposed carbonate rocks was found in Puding county, Guizhou

province (2005), accounting for 79.2 % of the county's total area. These carbonate rocks were mostly made up of Triassic, Permian dolomite, limestone, and argillaceous minerals. The weathering erosion rate of limestone only ranges from 23.7 to 110.7 mm/millennium (Chinese Academy of Sciences, Institute of Karst Geology Research Group 1979). Sample tests showed that chemical corrosion can hardly generate enough space to accommodate the lost soil. Shallow karst caves are normally filled, making the mechanism by which soil loss enters the underground karst space system difficult to elucidate. The improper human activities cause the vegetation destruction and aggravate the soil loss, which results in the acceleration of the karst rocky desertification (Drew 1983). The landforms in the watershed area of the Southern Yangtze River and Pearl River are mostly karst basin and peak cluster basin, whereas the landforms in the coastal area of the Northern Sancha River are mostly peak cluster depression and peak cluster canyon. The ecological environment is fragile, and the contradictory between human activities and land protection is very incisive. Moreover, serious karst soil loss and rocky desertification are caused by human activities. Since the 1950s, the rocky desertification area in Puding county increased, reaching 500 hm<sup>2</sup>/a in steep farming area, which is equivalent to 0.0013 hm<sup>2</sup>/a per capita of reduced cultivated land.

For the traditional theory cannot explain the underground accommodation space for the loss soil in the karst rocky desertification well, an erosion-creep-collapse mechanism of underground soil loss is presented with the evidence of investigation, experiment, and analysis in Chenqi village, Puding county, Guizhou China.

## Methodology

### Synthetical conceptual model establishment

In order to conceptualize the erosion-creep-collapse mechanism of underground soil loss for the karst rocky desertification, basic data and references are collected and analyzed in detail. The procedure of underground soil loss is presented with a clear evolution chain. Corresponding knowledges, including the geology, soil erosion, soil loss, soil mechanics, geochemistry and hazard geology, are combined and synthesized to understand and explain the underground soil loss procedure. Primary characteristics of the procedure are refined while the secondary factors are ignored. Typical characteristics of geological environment of typical karst slopes are summarized, the dynamic mechanism of underground soil loss is explained and the erosion-creep-collapse mechanism is proposed.



**Fig. 2** Land surface relief of karst hillside field

### Typical study area selection

Puding county, located in Southwest Guizhou province (Fig. 2) in Southwest China, is selected as the typical research area. It has a sub-tropical monsoon humid climate (Koppen Cfa), tempered by its low latitude and high elevation. It has fairly mild winters, warm summers, and a monsoon season. All year the climate is temperate, and the mean annual air temperature is 15.1 °C. The rainfall is abundant, and the mean annual rainfall is 1,378 mm. As a typical area with typical karst, lots of investigations and research works have been performed and lots of accumulated data and references can be gathered here. The former researches were performed focusing on karst, karst hydrogeology conditions, karst geochemistry and karst collapse, etc. The accumulated data are sythenticated authenticated, referred, and connected to support and explain the erosion-creep-collapse mechanism of underground soil loss.

### Investigation, sample collection, and experiment

Field investigation was performed by Tang and Yang etc. in 2008 and soil samples were collected in field. There are many surface tundishes, sinkholes, and karrens in the karst area of carbonate rock (Tang et al. 2010). These karst conformations could provide outlets for soil loss leakage (Yang et al. 2011a, b). Experiments, including shear strength tests, sieve tests, laboratory permeability test, and laboratory suction test, were designed and performed to obtain the particle size distribution, physical and mechanical properties, cultivation influence, etc. of soils.

Direct shear test (Das 2010) is adopted in shear strength test. The tests are designed for the surface soil of which the water content is from 30 to 40 %. Since the soil layer of the desertification area is very thin and poor, the cutting-ring samples are obtained from 15 cm below the surface, which are maintained by controlling water injection to get

different initial water contents in the tests. The vertical loadings are divided into three levels in different vertical location. There are two group tests to be carried out, and according to the site, each group test covers three samples with different water contents, respectively. In this test, the ZJ-type strain-controlling direct shear apparatus is adopted to apply the force.

In the sieve test, a set of standardized sieves (MHURC and GAQSIQ 1999) is used for the analysis. Each sieve is 200 mm in diameter and 50 mm in height. The particles are hand sieved using sieve sizes of: 0.075, 0.25, 0.5, 1.0, 2.0, 5.0, 10.0, 20.0, 40.0, and 60.0 mm. A dry soil specimen is then shaken through the sieves for 10 min. The percentage by weight of soil passing each sieve is plotted as a function of the grain diameter.

Constant-head test (Das 2010) is adopted in the laboratory permeability test. The water supply at the inlet is adjusted that the difference of head between the inlet and the outlet of a sample remains constant during the test period. After a constant flow rate is established, water is collected in a graduated flask for a known duration. Then the hydraulic conductivity can be calculated.

Osmotic method (controls matric suction) and vapor equilibrium technique (controls total suction) are adopted in laboratory suction test. In the osmotic method (Blatz et al. 2008) losses or uptakes of water are caused by the process of osmosis. The soil specimen is placed in contact with a semi-permeable membrane behind which an aqueous solution of large-sized polyethyleneglycol (PEG) molecules is circulated. Since water molecules can cross the membrane whereas PEG molecules cannot, an osmotic suction that increases with the PEG concentration is applied to the soil through the semi-permeable membrane. Since water transfer takes place in the liquid phase and ions can cross the semi-permeable membrane freely, the osmotic technique controls the matric suction of a soil and not the osmotic suction. In the vapor equilibrium technique (Blatz et al. 2008), a glass desiccator with a porous disk over the solution suspends soil specimens in the vapor environment above the chemical solutions. A net water exchange between the liquid and vapor phases occurs in the desiccator headspace until equilibrium between the two phases is achieved. The partial vapor pressure resulting due to the environment in the desiccator is directly a function of the concentration of the solution. Suctions are produced in soil specimens by the water exchange between the specimen and the vapor in the headspace of a desiccator.

### Mechanism verification and proof

As underground soil loss is a slow process, it will involve a lot of time and money to verify the mechanism and correct it. For there are lots of corresponding data can be referred



**Fig. 3** Overlying soil on karst slope

in the selected typical study area, the verifications of mechanism can be performed by detail analysis of the scraps of information.

### Geological environment of karst slopes

In this paper, the proposed erosion-creep-collapse mechanism of underground soil loss in karst slopes depends on a specific geological environment. The shallow geological characteristics of karst slopes are summarized as follows:

#### Undulating slope surface

The surface hypsography of karst slopes in rocky desertification is usually undulating. It contains many stone buds and steep slopes (Fig. 2). Their geomorphological character is not conducive to the preservation of soil and water. Soil movement easily occurs, leading to land rocky desertification (Wang 2002; Zhou et al. 2012a, b). For example, in the Puding karst mountain area in Guizhou, where rocky desertification develops seriously, the land surface is rugged and broken, the mountain area is very large, and several mountains with steep slopes exist. As a result, the loss of water, soil, and fertilizer is exacerbated, causing land rocky desertification (Zhang et al. 2011; Zhou et al. 2012a, b).

#### Undulating underlying bedrock surface with inhomogeneous soil

Soil loss, which leads to rocky desertification, mainly occurs on karst slopes and transitional areas between karst hillsides and depressions. The underlying bedrock surface fluctuates sharply for different surface and underground dissolutions (Sun et al. 2002a, b). Various scale joints,

fractures, and broken zones caused by tectonic stresses can be easily formed in carbonate rocks. Weathering appeared first at the fault areas and then numerous rock fractures and cave systems developed. Different weathering and dissolution patterns lead to the fluctuation of bedrock surface, where the surface elevation difference may reach several meters or even more than 10.00 m within a limited horizontal distance, and to the accumulation of inhomogeneous soil on low-lying areas (Fig. 3).

#### Overlying red soil

As the product of the karst process, red clay is widely distributed in carbonate rock areas. Several studies investigating the characteristics of red clay (Wang et al. 2002) have been done. Feng et al. (2002) indicated that red clay is composed of small and symmetrical porous particles with high natural water content, middle compressive ability, high strength, and impermeability, making it different from normal soils. Sun et al. (2002a, b) emphasized that soil and acid non-soluble substances migrate from high to low altitude places in micro or short distance (0.05–0.3 mm/a) under gravity and water force. Therefore, the soil erodes and migrates constantly in high-lying areas. However, it accumulates and forms residues in low-lying areas (Fig. 4) before it migrates to the space formed by differential erosion of carbonate rocks, such as underground depressions and rock fractures. The soil in high-lying areas gradually migrates to a nearby exposed bedrock.

#### Soil–rock interface providing channel for the lost soil

The lost soil enters the underground space through the soil–rock interface. The soil–rock interface can be divided into (1) the normal transition soil–rock interface and (2) the interface between the karst cave wall and the plunger soil,



**Fig. 4** Residual soil of karst hillside

which is the soil fill in the karst cave where the roof is broken. Normally, the lost soil needs to pass through the latter interface to form the channel through which the lost soil enters the underground space. The leakage interface introduced by (Zhang et al. 2007a, b) is the former one, whereas the latter is not mentioned.

#### Developed underground karst space accommodating the lost soil

Underground karst is developed where clint and depression are distributed. Underground karst caves without roof are usually filled with soil. The size of the karst caves are about 0.1–5.0 m in diameter and 0.0–15.0 m in depth. The area of clint and depression is 1.48, 0.695 km<sup>2</sup>, respectively. The density of the funnel of clint and depression is 8.4 and 6.2 ind/km<sup>2</sup>, respectively (Zhang et al. 1996). In karst caves, the areas where roof parts collapse are filled with soil or collapse rocks in the window. Thus, channels that can accommodate the lost soil are hardly provided. By contrast, the areas where roof parts are still intact contain unfilled spaces. Once the filled channel is dredged, it will provide enough space to accommodate the lost soil.

#### Water table lying under the soil bottom providing erosion and transport force

Karst slopes and hillside fields often have deep groundwater table that lies under the soil bottom (Fig. 5). The rainfall that penetrates the underground system through the soil provides necessary conditions for soil loss and scouring effect. The karst hydraulic system in Southwest China has a special dual structure, through which rainfall can easily enter the underground river from the steep slope, fracture, and slocker, and then drain from the deep gorge to the river. The soil-up and groundwater-down patterns are formed and frequently lead to temporary drought (Han

2002). The soil is thin, non-continuous with weak water holding capacity.

### Dynamic mechanism of underground soil loss

#### Soil structure destroyed by human cultivation

Soil structure destroyed by human cultivation provides the necessary basis for underground soil loss of karst slopes and hillside fields (Fig. 6). The county-wide jurisdiction in Puding county, Guizhou province, China (2005) is a typical example. In the Puding county, carbonate rocks are widely distributed, and approximately 863.7 km<sup>2</sup> (about 79.2 % of the county's territory) is exposed; the land area which is suitable for cultivation is limited. This limited land area is then fully cultivated by local people as a mean of life and as a result, the structure of rigid soil is damaged and the strength and stability of the soil is decreased. Consequently, surface water penetrates into the soil easily, providing the preconditions for the underground soil loss.

Laboratory tests were performed to verify the influence of cultivation on soil strength. Soil samples were collected from Chenqi village, Puding county, Guizhou province, China. In order to reflect the change of the water content after rainfall, water injection treatments were made to the undisturbed samples to control the saturation levels to 80, 90, and 100 % of the actual water content. To ensure saturation of moisture of the soil, samples were treated for 48 h. According to the liquid limit and plastic limit of the clay, the remolded samples were designed with three different water contents, which are 30, 35, and 40 %. There were two group tests to be carried out, and according to the site, each group test covered three typical samples with different water contents, respectively. The variation in shear strength of the soil mass with different water contents was obtained to interpret the process of the underground soil loss model. The variations in the cohesive force and internal friction angle of undisturbed and remolded (soil that has had its natural internal structure modified or disturbed by manipulation) samples with different water contents obtained from the direct shear test are shown in Figs. 7 and 8. The results indicate that soil cohesive force and internal friction angle decrease with the increase in the water content. As shown in the figures, the soil cohesive force and internal friction angle of the disturbed samples are lower than those of the undisturbed samples. From Fig. 7, it can be seen that with the increase in the water content, the cohesive stress of the brown clay gradually decreases and the properties of the soil move more close to the sandy soil. Meanwhile, the relationship between the shear strength of the undisturbed samples and the water content is closely linear. The variation in cohesive force in

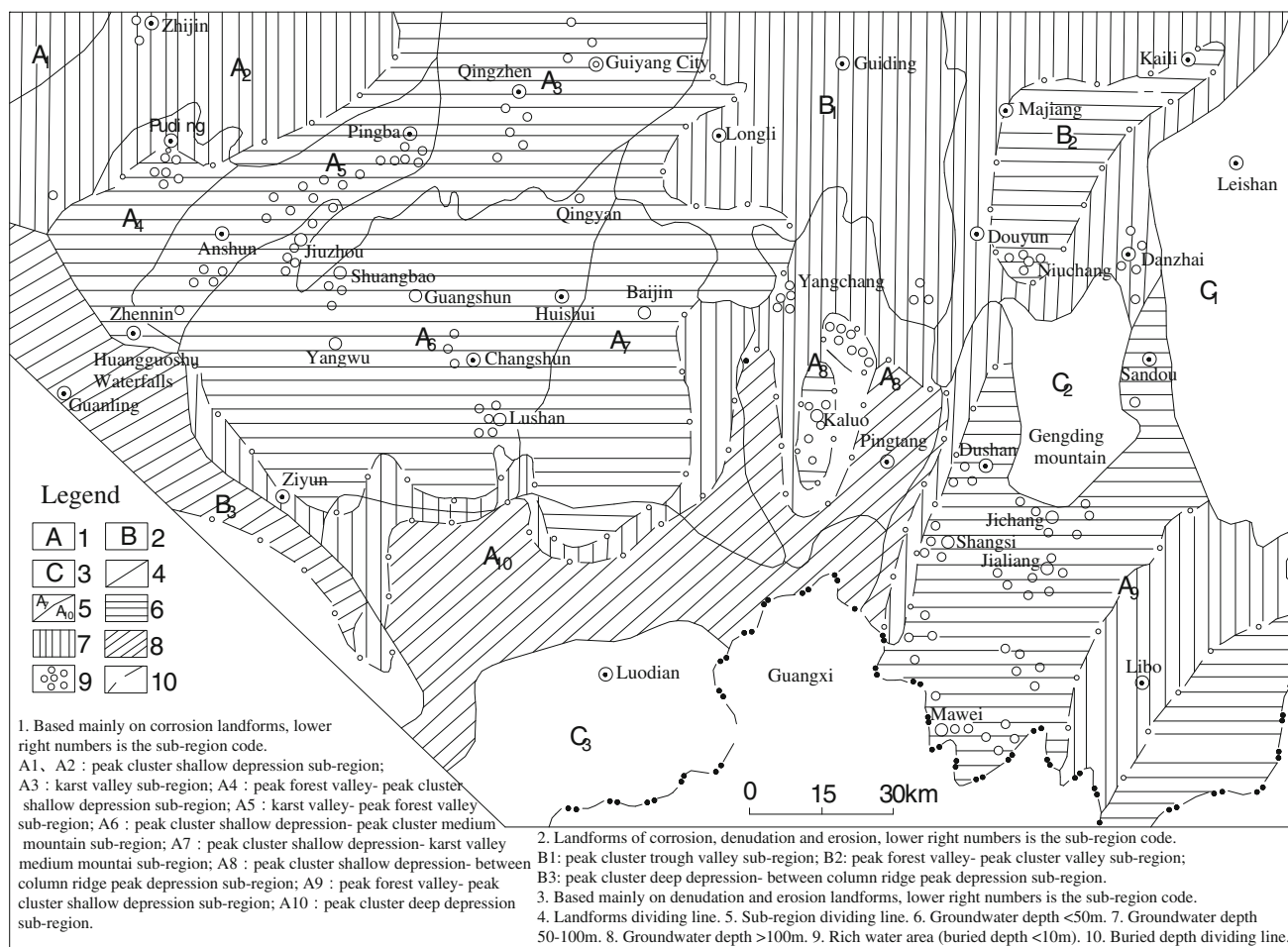


Fig. 5 Depth of groundwater table and karst geomorphology in Guizhou province (Gao et al. 1985)



Fig. 6 Human cultivation activities on the thin cover soil layer

remolded samples is much larger than that in undisturbed samples. In contrast, the variation in the internal friction angle is similar with the cohesive force (Fig. 8). It can also be seen that the strength parameters of the brown clay directly correlated with the water content, either in the undisturbed samples or in the remolded samples. The

weakening of particle bonds with the increase in the water content is apparent. As can be seen in Fig. 9, the hydraulic conductivities of shallow sample are bigger than that of the deep one. With the decrease in the soil depth, the hydraulic conductivities increase sharply. Soil permeability increases sharply in shallow areas because of human cultivation

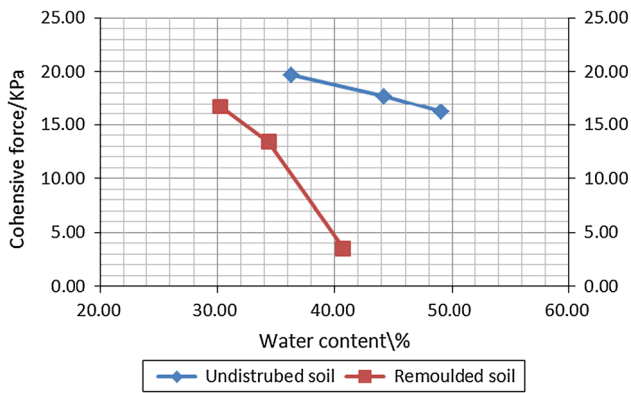


Fig. 7 Cohesive force of soil sampled in Puding county

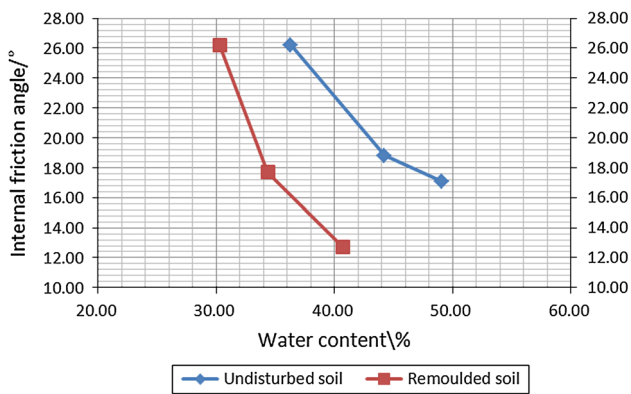


Fig. 8 Internal friction angle sampled in Puding county

activities. The data indicate that irrigation and cultivation can decrease soil strength obviously, which proves that karst soil erosion and loss are closely related to human activities. According to the statistical data obtained from the administrative division, population density is positively correlated with the distribution of underground soil loss and rocky desertification. The denser the population density, the wider the soil loss and rocky desertification. The average population density of Puding county is 366 people/km<sup>2</sup>, which is the largest population density in Guizhou province and far beyond the reasonable capacity under the current undeveloped productive force level. The population overload rate exceeds over 40%. The problem of food and clothing as well as cultivated steep slopes leads to a vicious circle of increasing population–excess cultivation–land degradation–impoverished economy. Overload graving also speeds up rocky desertification. At present, the whole rocky desertification area caused by soil loss has reached 399.14 km<sup>2</sup> (not including the latent rocky desertification area), which is 36.6% of its territory (46.2% area of exposed carbonate rocks). Mild, moderate, strong, and extremely strong rocky desertification areas account for 13.9, 14.9, 6.8, and 0.9% of the total area, respectively.

The area above the moderate rocky desertification accounts for 22.7% of the country’s territory (Puding county of Guizhou province 2005), with a bare crag area taking above 50% of it.

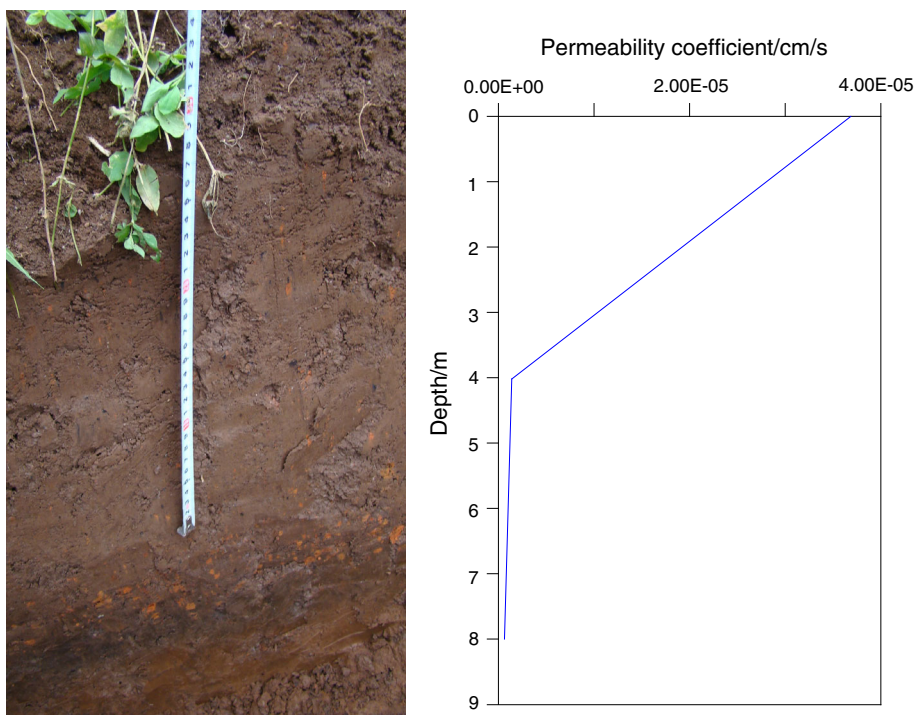
#### Underground runoff from rainfall

In 2007, Institute of geochemistry, Chinese academy of sciences, established the six runoff plots in Chenqi village, Puding county (Peng et al. 2008). It demonstrated that the surface runoff can penetrate into the underground easily in karst areas. After continuous in situ monitoring of soil loss, six runoff plots with different kinds of land usage (shrub-grass, burning grass, secondary forest, slope farmland, shrubbery land and tree and shrub) on karst slope, and groundwater level in the outlet of the catchment of Chenqi village, Puding county were established. The result indicates that the runoff coefficient (the percentage of rainfall that appears as stormwater run-off from a surface) of the six runoff plots is very small (between 0.01 and 12.81%). Most of the surface runoff penetrates into the underground runoff, making the production of efficient surface runoff in the karst hillside field difficult (Fig. 10). Given that the water table is beneath the soil bottom, a huge amount of water from rainfall is transferred to the underground runoff with the influence of human activities. In this process, the infiltrated water has to seep into the soil as pore groundwater before reaching the karst cave groundwater system. As a result, a large hydraulic gradient in the soil is reached, causing long-term soil loss and underground soil loss. This phenomenon may lead to the development of a soil pipe. Once the soil pipe extends to the ground surface and collapses, more soil will migrate into the karst cave. Experiments on monitoring surface runoff, suspensional sediment yield, and soil loss for each rainfall event were carried out in six runoff fields with different land use types, using large slope runoff field method, in Chenqi catchment, from July 2007 to December 2008 (Peng et al. 2009). The results show that annual soil loss and suspensional sediment yield in six runoff fields vary greatly, from 0.05 to 62.25 t/km<sup>2</sup> and 0.03 to 8.68 t/km<sup>2</sup>, the largest one occurs in the sparse shrubs runoff field which is classified as moderate rocky desertification. Soil loss in karst slopes generally occurs in heavy rainstorms where the precipitation exceeds 60 mm. Though the surface runoff is the dominating factor of soil loss, it is also being affected by rainfall characteristic and vegetation cover.

#### Wet–dry cycle

The long-term dry/wet cycling process caused by the climate change induces a continuously compaction and degradation of the cultivated soil in karst rocky desertification

**Fig. 9** Permeability with depth in Puding county, Guizhou province



areas. The laboratory cyclic wet–dry tests were conducted on undisturbed and disturbed soil to study the effect of the water content. In suction-controlled wet–dry tests, two suction control methods are used: the osmotic method for low suction range (0.05–1 MPa) and the vapor equilibrium technique for high suction range (9–309 MPa). At each suction level, water content of undisturbed and disturbed soil specimen is determined after the equilibrium is reached. The values of suction and the corresponding water content are shown in Table 2. The results indicate that suction decreases with the increase in the water content. The soil cohesive force and internal friction angle decrease with the increase in the water content (Figs. 7, 8). In the course, the shear strength in the soil is weakened, causing underground soil loss. Ye et al. (2011) analyzed the mechanism of cultivation soil degradation in rocky desertification areas under dry/wet cycles. The results show that under the effect of dry/wet cycles, (1) the void ratio of the cultivated soil decreases continuously, leading to a gradual soil compaction and (2) the permeability decreases, giving a rise to a deterioration of water transfer ability as well as a deterioration of soil–water retention capacity.

#### Underground soil erosion

The uniformity coefficient ( $C_u$ ) can be used to determine the type of the soil loss failure. Flow soil occurs when  $C_u$  is less than 10, while piping effect occurs when  $C_u$  is larger

than 20. If the value of  $C_u$  is larger than 10 but smaller than 20, both the flow soil and piping effect may occur.

The physical properties of the undisturbed soil in Chenqi village, Puding county, Guizhou province, are shown in Table 3. The sieve distribution curves inside and outside the karst cave are shown in Figs. 11 and 12, respectively.

The  $C_u$  outside the karst cave is given in Eq. (1) (MHURC and GAQSIQ 2008), and the obtained value shows that piping may occur:

$$C_u = \frac{d_{60}}{d_{10}} = \frac{0.5}{0.01} = 50, \tag{1}$$

where  $d_{60}$  is the limited size, and  $d_{10}$  is the effective size.

The  $C_u$  inside the karst cave is given in Eq. (2) (MHURC and GAQSIQ 2008), and the obtained value indicate that piping or soil flow may be produced.

$$C_u = \frac{d_{60}}{d_{10}} = \frac{0.018}{0.0015} = 12. \tag{2}$$

The critical hydraulic gradient of piping type or transitional type can be calculated using the following equation (MHURC and GAQSIQ 2008):

$$J_{cr} = 2.2(G_s - 1)(1 - n)^2 \frac{d_5}{d_{20}}, \tag{3}$$

where  $J_{cr}$  is the critical hydraulic gradient,  $G_s$  is the grain weight,  $n$  is the original porosity,  $d_5$  is the diameter (mm) through which 5 % of the soil particles pass, and  $d_{20}$  is the diameter (mm) through which 20 % of the soil particles pass.



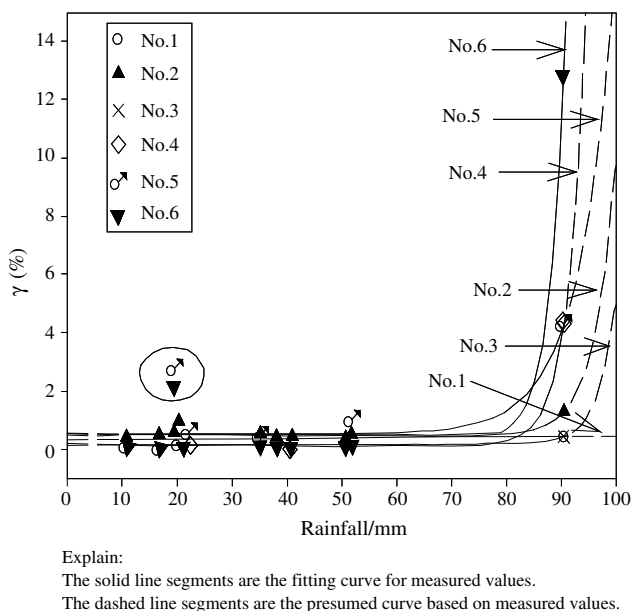


**Fig. 10** Evidence of surface runoff (Peng et al. 2008)

According to the equation shown above, the critical hydraulic gradient can be calculated.

For soil outside the karst cave

$$J_{cr} = 2.2 \times (2.44 - 1) \times \left(1 - \frac{1.20}{1 + 1.20}\right)^2 \times \frac{0.0015}{0.08} = 0.015. \tag{4}$$

For soil inside the karst cave

$$J_{cr} = 2.2 \times (2.44 - 1) \times \left(1 - \frac{1.20}{1 + 1.20}\right)^2 \times \frac{0.006}{0.08} = 0.063. \tag{5}$$

Considering the structure of the upper soil and lower water, when the underground water penetrates into the soil body and flows out at the outlet of the seepage, the

hydraulic gradient probably reaches 1. In this case, the underground erosion is very easy to occur. The fine particles are removed because of the underground erosion, and soil loss occurs immediately. Simultaneously, soil pipes are produced in the growing pore space to accommodate the soil coming from the upper space.

### Underground soil creeping

High and unsaturated soil clay contents cause the soil body to be very hard. The tucking action of the filled earth pillars and the crag immobilizes the soil with low water contents. This phenomenon is called the plunger effect of the soil. The soil test results of the field samples showed that the soil in Chenqi village, Puding county, Guizhou province, is in a plastic state (Fig. 13; Table 4). Concentrated underground runoff will be formed after rainfall. The underground water table increases because of the structure of the upper soil and lower water. Rainwater enters the underground karst system only through the filled soil body. When the water content increases to the liquid limit, the soil is in a soft plastic state or flow plastic state. No binding effect is found between the soil body and the unfilled space of the filled soil in the cave. The soil makes contact with plastic flow, causing the creeping movement of the whole plunger soil body and providing the necessary conditions for the partition of the internal pipe and the incumbent stratum.

### Karst collapse

When the underground soil loss develops to a certain degree, the soil is in the limit equilibrium state. The collapse occurs under the trigger action in material transportation. When the above process is repeated many times, the soil collapses into the underground space, leading to a continuous development of soil leakage.

### Erosion-creep-collapse mechanism of underground soil loss

According to the geological characteristics of hillside fields and the analysis of the collapse dynamic mechanism, the erosion-creep-collapse dynamic mechanism of underground soil loss is proposed in this paper (Fig. 14). Seven stages of the established karst underground soil loss dynamic mechanism are discussed as follows:

1. In the natural process, the partial destruction and absence of the karst cave roof induce the downward movement of the soil body. As a result of the plunger effect of earth pillars, the cave is filled and no space for

**Fig. 11** Particle sieve distribution curve outside the karst cave

| Particle diameter (cm) | Particles finer than a given sieve (%) |
|------------------------|--|
| 0.9000                 | 99.20                                  |
| 0.5000                 | 57.70                                  |
| 0.2500                 | 36.83                                  |
| 0.1000                 | 25.97                                  |
| 0.0740                 | 21.10                                  |
| 0.0551                 | 15.89                                  |
| 0.0390                 | 15.05                                  |
| 0.0247                 | 13.80                                  |
| 0.0143                 | 11.71                                  |
| 0.0101                 | 10.45                                  |
| 0.0072                 | 9.62                                   |
| 0.0051                 | 8.78                                   |
| 0.0015                 | 6.27                                   |

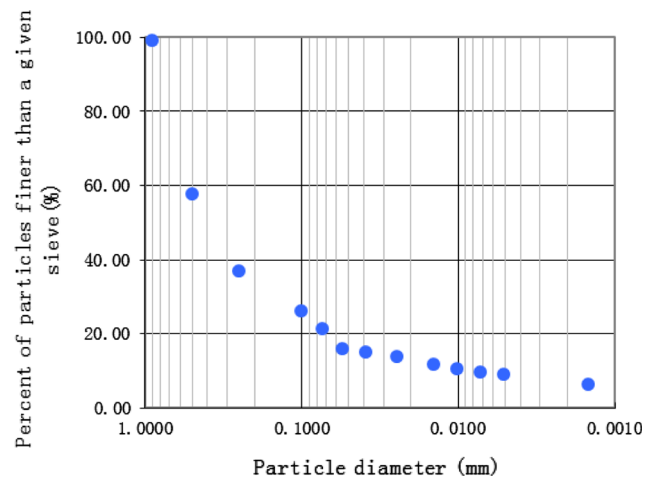


**Table 2** Suction and the corresponding water content

| Methods                     | Saturated salt solution                              | Suction (MPa) | Disturbed soil Water content (mean value) (%) | Undisturbed soil Water content (mean value) (%) |
|-----------------------------|--|---------------|---|---|
| Vapor equilibrium technique | LiCl·H <sub>2</sub> O                                | 309           | 3.16  | 5.46  |
|                             | K <sub>2</sub> CO <sub>3</sub>                       | 113           | 3.43  | 6.40  |
|                             | Mg(NO <sub>3</sub> ) <sub>2</sub> ·6H <sub>2</sub> O | 82            | 4.19  | 7.42  |
|                             | NaNO <sub>2</sub>                                    | 57            | 4.93  | 9.30  |
|                             | (NH <sub>4</sub> ) <sub>2</sub> SO <sub>4</sub>      | 24.9          | 6.70  | 10.83   |
|                             | KNO <sub>3</sub>                                     | 9             | 10.68   | 17.74   |
| Osmotic method              |  | 1             |   | 35.06   |
|                             |  | 0.5           | 23.73   | 39.76   |
|                             |  | 0.2           | 30.86   | 42.49   |
|                             |  | 0.1           |   | 44.05   |
|                             | 0.05   | 33.69         | 45.50   |   |

the covered soil layer to move downward is allowed (Fig. 14a).

- Human cultivation activities, vegetation damage, and planting activities cause the structure of the cap soil to become loose. After rainfall, the ground surface water accumulates and penetrates into the karst cave, forming the seepage flows in the filled soil. The soil body reaches the critical state after rainfall in the first stage of the soil dropout. The concentrated penetration makes the filled material in the karst cave corrode, erode, and creep, resulting in the loss of the filled material and local free surface formation in the filled material (Fig. 14b).
- The filled material in the cave erodes and creeps gradually in the wet–dry cycle because of the rainfall. The free surface moves upward, whereas the filled soil in the cave stays stable because of the friction generated by the plunger effect (Fig. 14c).
- As the free surface ascends, the lower filled material creeps and separates from the covered soil layer, and then forms a hole near the karst cave (Fig. 14d).
- The hole gradually develops upward, reaches the state of limit equilibrium, and develops to the ground surface (Fig. 14f).
- Collapse occurs, and soil transportation stops (Fig. 14e).

**Table 3** Physical properties of the undisturbed soil of Chenqi village, Puding county, Guizhou province

| Soil type | Soil depth (cm) | Project | Water content (%) | Void ratio | Density (g/cm <sup>-3</sup> ) | Saturation (%) |
|-----------|-----------------|---------|-------------------|------------|-------------------------------|----------------|
| Red clay  | 0–15            | Maximum | 37.00             | 1.00       | 1.532                         | 75.53          |
|           |                 | Minimum | 32.03             | 1.43       | 1.833                         | 85.58          |
|           |                 | Average | 38.86             | 1.20       | 1.440                         | 80.09          |

**Fig. 12** Particle sieve distribution curve inside the karst cave

| Particle diameter (mm) | Particles finer than a given sieve (%) |
|------------------------|--|
| 0.9000                 | 99.93                                  |
| 0.5000                 | 98.67                                  |
| 0.2500                 | 93.53                                  |
| 0.1000                 | 83.73                                  |
| 0.0740                 | 77.43                                  |
| 0.0516                 | 73.43                                  |
| 0.0366                 | 70.87                                  |
| 0.0233                 | 65.73                                  |
| 0.0137                 | 52.89                                  |
| 0.0098                 | 37.49                                  |
| 0.0070                 | 27.22                                  |
| 0.0050                 | 16.95                                  |
| 0.0015                 | 9.24                                   |

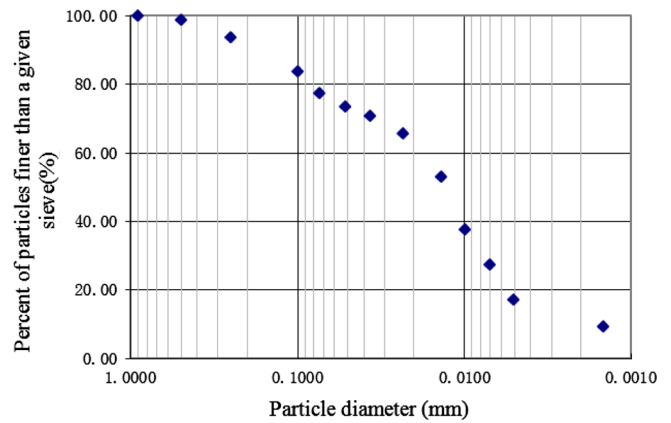
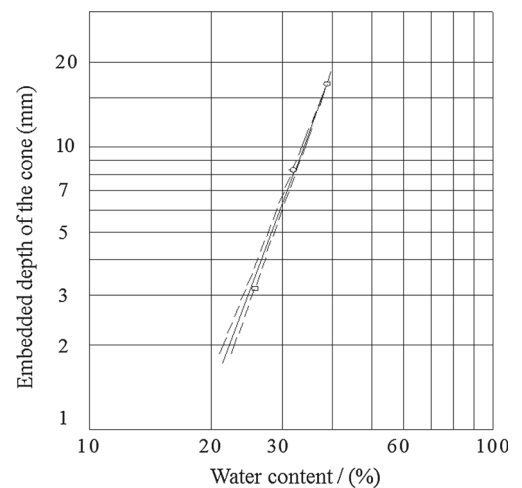


**Fig. 13** Plastic index and liquid index of Chenqi village, Puding county, Guizhou province

|                        |       |         |
|------------------------|-------|---------|
| Plasticity index $I_p$ | 10 mm | 11.6843 |
|                        | 17 mm | 16.7558 |
| Liquidity index $I_L$  | 10 mm | 0.5833  |
|                        | 17 mm | 0.40675 |



7. The hole formed by the collapse is razed under weathering and gravity, and the cave is filled (Fig. 14g).

There are many evidences to prove the erosion-creep-collapse dynamic mechanism. Sun et al. (2002a, b) demonstrated that the surface soil can be taken to the deep accumulation space by the groundwater. The thick clay

layer in the caves can also prove that the surface soil material could be taken away and deposited at underground caves (Soil survey office of Guizhou province 1994; Lewis 1995; Hardwick and Gunn 1990, 1996). Zhang et al. (2009) found a thick layer of red clay deposits in the karst cave of Western Guizhou. According to the concentration testing results of the profile, the upper red clay is considered to be

brought from the ground surface. Wei et al. (2010) studied soil surface loss and underground soil loss with  $^{137}\text{Cs}$  technique. The results show that the soil moved downward along the slope in the barren land of the karst mountain valley area while the soil moved down the profile because of the existence of soil loss in the vegetable, breaking the law of soil down together. Wan and Bai (1998) used the

cosmogenic nuclide  $^7\text{Be}$  for carbonate regional tracer study and found that most soil particles from carbonate rock areas are moved in micro area or in short range. In fact, the undulating macro and micro topography of karst regions also limits the long-distance transportation of surface soil particles. They also found that limestone soil can disappear from the surface without long-distance transportation. The accumulation of surface soil in the rock fracture or its migration to the underground caves is an important cause of material loss. To investigate the loss mechanism of karst areas, several researchers proposed the distinct concept of soil loss. Previous studies on lichens, pollen, and morphology of limestone dissolution confirmed the universality of short-distance soil loss in karst areas (Trudgill 1985; Li et al. 2001).

**Table 4** Consistency state determined by liquid index of clay

| Liquid index ( $I_L$ ) value | Consistency state |
|------------------------------|-------------------|
| $I_L \leq 0$                 | Hard              |
| $0 < I_L \leq 0.25$          | Hard plastic      |
| $0.25 < I_L \leq 0.75$       | Plastic           |
| $0.75 < I_L \leq 1$          | Soft plastic      |
| $1 < I_L$                    | Flow plastic      |

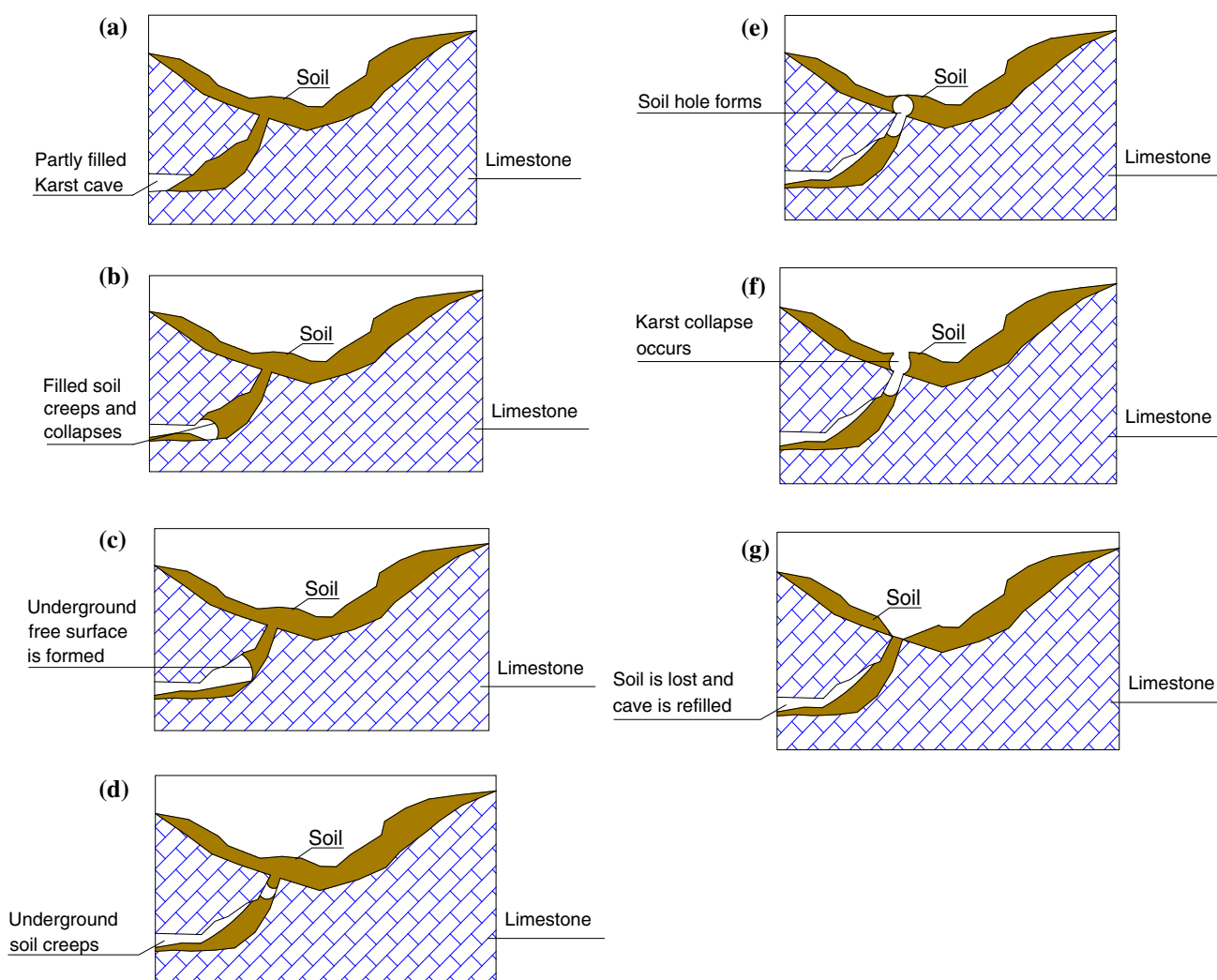


**Fig. 14** Erosion-creep-collapse dynamic mechanism of Karst hillside field. **a** Underground cave is partly filled. **b** Filled material creeps and is transported by internal erosion. **c** Free surface develops upward.

**d** Internal soil becomes unstable and begins to creep. **e** Soil hole develops to the ground surface. **f** Soil hole collapses. **g** Ground surface collapses and slopes are razed

## Conclusions

1. In China, carbonate rocks are widely distributed, and karst soil loss has created a wide range of land rocky desertification. Field monitoring indicated that underground leakage is the major mechanism of karst soil loss and that it occurs without obvious ground outflow. However, surface soil creeping to the underground space needs a connective space. Usually, the cave near the ground surface with exposed roof is filled with soil. The previous researches failed to explain fully the mechanism and problems of the formation of underground space.
2. An erosion-creep-collapse mechanism of karst underground soil loss is proposed. The mechanism is part of the mechanisms of karst soil loss, which will occur under the following geological background: large surface hypsography, significantly fluctuating of underlying bedrock surface, thin and inhomogeneous incumbent soil clays, incumbent soil clays and bedrock with product relations, grown underground karst, soil-rock interface, deep groundwater table with water lying under soil clays and partly filled karst underground caves.
3. The major power of dropout mainly stems from human cultivation activities that destroy the soil structure. The runoff generated from rainfall provides underground hydraulic power. The wet–dry cycle is also generated from rainfall. The erosion effect is caused by rainfall penetration. Creeping of plastic-stream soil and land subsidence are also observed.
4. The seven stages of erosion-creep-collapse mechanism of underground soil loss are proposed: filled cave disturbance by human activities, internal corrosion and potential collapse, formation of free surfaces within the soil body, internal soil creeping, soil pipe formation, soil pipe collapse, and ground surface collapse and filling.
5. This mechanism is slow–sudden change transportation. It indicates that underground soil loss can be governed by controlling human activity and that soil collapse can be prevented; thus the large-scale stone desertification of karst hillside fields can be avoided.

**Acknowledgments** This work is supported by the National Natural Science Foundation of China (No. 41072205), the research Grant (No. 201311045-04) from the Special Fund for Land and Resources- scientific Research in the Public Interest of China, the Key Discipline Construction Program of Shanghai (Geological Engineering, No. B308) and the Foundation of China Railway No. 2 Engineering Group Co., Ltd. (No. 201218). The authors wish to thank Dr. Tian Qian from Nanyang Technological University for his kind suggestion and the discussions for this paper.

## References

- Anselmetti FS, Hodell DA, Ariztegui D, Brenner M, Rosenmeier MF (2007) Quantification of soil erosion rates related to ancient Maya deforestation. *Geol* 35:915–918
- Blatz JA, Cui Y, Oldecop L (2008) Vapour equilibrium and osmotic technique for suction control. *J Geotech Geol Eng* 26:661–673
- Chen X, Zhang Z, Chen X, Shi P (2009) The impact of land use and land cover changes on soil moisture and hydraulic conductivity along the karst hillslopes of Southwest China. *Environ Earth Sci* 59:811–820
- Chinese academy of sciences, institute of karst geology research group (1979) *China karst studies*. Geological Publishing House, Beijing (in Chinese)
- Das BM (2010) *Principles of geotechnical engineering*, 7th edn. Cengage Learning, Stamford
- Drew DP (1983) Accelerated soil erosion in a karst area: the Burren, western Ireland. *J Hydrol* 61:113–124
- Febles JM, Tolon A, Vega MB (2009) Edaphic indicators for assesment of soil erosion in karst regions, province of Havana Cuba. *Land Degrad Develop* 20:522–534
- Febles-González JM, Vega-carreño MB, Tolón-Becerra A, Lastra-Bravo X (2012) Assessment of soil erosion in karst regions of Havana Cuba. *Land Degrad Develop* 23:465–474
- Feeser I, O’Connell M (2009) Fresh insights into long-term changes in flora, vegetation, land use and soil erosion in the karstic environment of the Burren, western Ireland. *J Ecol* 97:1083–1100
- Feng Z, Wang S, Sun C, Liu X (2002) Practical index to distinguish the origin of earthy deposits in karst area-characteristics of grain size distribution. *Carsologica Sin* 2:3–8 (in Chinese)
- Gao D, Zhang S, Sheng X, Dong C, Wu Z, Nie Y (1985) *Karst research in south Guizhou province*. Guizhou People’s Publishing House, Guiyang (in Chinese)
- Geissen V, Kampichler C, López-de Llergo-Juárez JJ, Galindo-Acántara A (2007) Superficial and subterranean soil erosion in Tabasco, tropical Mexico: development of a decision tree modeling approach. *Geoderma* 139:277–287
- Han G (2002) Characteristics of natural and human processes of karst changes in environmental quality-geochemistry of karst rivers in Guizhou. Dissertation, Institute of Geochemistry in Chinese Academy of Sciences (in Chinese)
- Hardwick P, Gunn J (1990) Soil erosion on cavernous limestone catchment. In: Boardman J, Foster I, Dearing J (eds) *Soil erosion on agricultural land*. John Wiley, Chichester, pp 301–310
- Hardwick P, Gunn J (1996) Modern fluvial processes on a macroporous drift covered cavernous limestone hillslope, Castleton, Derbyshire, UK. In: Anderson M, Gand Brooks SM (eds) *Advances in hillslope processes*. John Wiley, Chichester, pp 397–428
- Huang Q, Cai Y (2007) Spatial pattern of karst rock desertification in the Middle of Guizhou province, Southwestern China. *Environ Geol* 52:1325–1330
- Jiang Z, Lian Y, Qin X (2013) Carbon cycle in the epikarst systems and its ecological effects in South China. *Environ Earth Sci* 68:151–158
- Kheir RB, Abdallah C, Khawlie M (2008) Assessing soil erosion in Mediterranean karst landscapes of Lebanon using remote sensing and GIS. *Eng Geol* 99:239–254
- Lewis S (1995) Clear cutting on karst: soil erodes into limestone caves. *Watershed Sentin* 5:119–127
- Li D, Cui Z, Liu G, Feng G, Cao J (2001) Formation and evolution of karst weathering crust on limestone and its cyclic significance. *Carsologica Sin* 3:17–22 (in Chinese)

- Ministry of Housing and Urban-Rural Construction of the People's Republic of China (MHURC), General Administration of Quality Supervision, Inspection and Quarantine of the People's Republic of China (GAQSIQ) (2008) Code for engineering geological investigation of water resources and hydropower. China Planning Press, Beijing (in Chinese)
- Ministry of Housing and Urban-Rural Construction of the People's Republic of China (MHURC), General Administration of Quality Supervision, Inspection and Quarantine of the People's Republic of China (GAQSIQ) (1999) Standard for soil test method (GB/T 50123-1999). China Planning Press, Beijing (in Chinese)
- Peng J, Cai Y, Yang M, Liang H, Liang F, Song L (2007) Relating aerial erosion, soil erosion and sub-soil erosion to the evolution of Lunan Stone Forest China. *Earth Surf Process Landf* 32:260–268
- Peng T, Wang S (2012) Effects of land use, land cover and rainfall regimes on the surface runoff and soil loss on karst slopes in Southwest China. *Catena* 90:53–62
- Peng T, Wang S, Zhang X, Rong L, Yang T, Chen B, Wang J (2008) Results of preliminary monitoring of surface runoff coefficients for karst slopes. *Earth Environ* 36:125–129 (in Chinese)
- Peng T, Yang T, Wang S, Zhang X, Chen B, Wang J (2009) Monitoring results of soil loss in karst slopes. *Earth Environ* 37:126–130 (in Chinese)
- Puding county of Guizhou province (2005) Comprehensive prevention planning of rocky desertification of Puding county (in Chinese)
- Soil survey office of Guizhou province (1994) The soil in Guizhou province. Guizhou Science and Technology Press, Guiyang (in Chinese)
- Sun C, Wang S, Liu X, Feng Z (2002a) Geochemical characteristics and formation mechanism of rock-soil interface in limestone weathering crust at Huaxi, Guizhou province. *Acta Mineralogica Sin* 2:126–132 (in Chinese)
- Sun C, Wang S, Zhou D, Li R, Li Y (2002b) Differential weathering and pedogenetic characteristics of carbonate rock sand their effect on the development of rock desertification in karst regions. *Acta Miner Sin* 22:308–314 (in Chinese)
- Tang Y, Zhang X, Zhou J, She T, Yang P, Wang J (2010) The mechanism of underground leakage of soil in karst rocky desertification areas—a case in Chenqi small watershed, Puding, Guizhou province. *Carsologica Sin* 29:121–127 (in Chinese)
- Trudgill S (1985) Limestone geomorphology. Longman Group Limited, London
- Vega MB, Febles JM (2008) Application of the new method of evaluation of the soil erosion (EVERC) and the model MMF in soils of the Mamposton cattle production basin in Havana province Cuba. *Cuban J Agric Sci* 42:299–304
- Wan G, Bai Z (1998) Research on the carbonate rock erosion and environmental change—a case study in south Guizhou. *Quat Res* 18:279–286 (in Chinese)
- Wang B, Yang S, Lue C, Zhang J, Wang Y (2010) Comparison of net primary productivity in karst and non-karst areas: a case study in Guizhou province, China. *Environ Earth Sci* 59:1337–1347
- Wang S (2003) The most serious ecogeologically environmental problem in Southwestern China—karst rocky desertification. *Bull Miner Petrol Geochem* 22:120–126 (in Chinese)
- Wang S, Sun C, Feng Z, Liu X (2002) Mineralogical and geochemical characteristics of the limestone weathering profile in Jishou, western Hunan province, China. *Acta Miner Sin* 22:19–29 (in Chinese)
- Wang S (2002) Concept deduction and its connotation of karst rocky desertification. *Carsologica Sin* 21:101–105 (in Chinese)
- Wei X, Yuan D, Xie S (2010) Study on soil erosion and loss on slope in karst mountain valley area of chongqing valley with <sup>137</sup>Cs and soil nutrient elements. *J Soil Water Conserv* 24:16–19 (in Chinese)
- Xu Y, Peng J, Shao X (2009) Assessment of soil erosion using RUSLE and GIS: a case study of the Maotiao River watershed, Guizhou province, China. *Environ Geol* 56:1643–1652
- Xu Y, Luo D, Peng J (2011) Land use change and soil erosion in the Maotiao River watershed of Guizhou province. *J Geogr Sci* 21:1138–1152
- Xu Y, Shao X, Kong X, Peng J, Cai Y (2008) Adapting the RUSLE and GIS to model soil erosion risk in a mountains Karst watershed, Guizhou province, China. *Environ Monit Assess* 141:275–286
- Yang P, Tang Y, Zhou NQ, Wang J, She T, Zhang X (2011a) Characteristics of red clay creep in karst caves and loss leakage of soil in the karst rocky desertification area of Puding county, Guizhou, China. *Environ Earth Sci* 63:543–549
- Yang Q, Wang K, Zhang C, Yue Y, Tian R, Fan F (2011b) Spatio-temporal evolution of rocky desertification and its driving forces in karst areas of Northwestern Guangxi, China. *Environ Earth Sci* 64:383–393
- Yang Z, Yang L, Zhang B (2010) Soil erosion and its basic characteristics at karst rocky-desertified land consolidation area: a case study at Muzhe village of Xichou county in Southeast Yunnan. *China J Mt Sci* 7:55–72
- Ye W, Qi Z, Chen B, Xie J, Huang Y, Lu Y, Cui Y (2011) Mechanism of cultivation soil degradation in rocky desertification areas under dry/wet cycles. *Environ Earth Sci* 64:269–276
- Zhang X, Bai X, He X (2011) Soil creeping in the weathering crust of carbonate rocks and underground soil losses in the karst mountain areas of Southwest China. *Carbonate Evaporite* 26:149–153
- Zhang X, Bai X, Wen A (2010) Preliminary investigation of the potential for using the <sup>137</sup>Cs technique to date sediment deposits in Karst depressions and to estimate rates of soil loss from Karst catchments in Southwest China. In: Banasik K et al (ed) *Sediment dynamics for a changing future*, Iahs Publ. vol 337. Wallingford, pp 149–156
- Zhang X, Wang S, Cao J (2009) Mass balance of silicate minerals in soils and soil losses in the karst mountainous regions of Southwest China. *Earth Environ* 37:97–102 (in Chinese)
- Zhang X, Wang S, He X, Wang Y, He Y (2007a) Soil creeping in weathering crusts of carbonate rocks and underground soil losses on karst slopes. *Earth Environ* 35:202–206 (in Chinese)
- Zhang X, Wang S, He X, Wang Y, Wen A (2007b) A preliminary discussion on the rocky desertification classification for slope land in karst mountain areas of Southwest China. *Earth Environ* 35:188–192 (in Chinese)
- Zhang Z, Yang J, Wang X, Shen P (1996) Classification and characters of karst surface spatial structure in Puding Guizhou. *J Nanjing Univ* 32:302–308 (in Chinese)
- Zhou J, Tang Y, Yang P, Zhang X, Zhou N, Wang J (2012a) Inference of creep mechanism in underground soil loss of Karst conduits I Conceptual model. *Nat Hazards* 62:1191–1215
- Zhou J, Tang Y, Zhang X, She T, Yang P, Wang J (2012b) The influence of water content on soil erosion in the desertification area of Guizhou, China. *Carbonate Evaporite* 27:185–192